

EVALUATION OF SPATIOTEMPORAL CHARACTERISTICS OF PRECIPITATION EXTREMES VARIATIONS IN AMUR RIVER BASIN

YAN, B.¹ – XU, J.¹ – WANG, Y.^{1*} – HUANG, F.² – HAN, X.¹ – ZHANG, L.³ – GUO, L.⁴

¹*Changjiang River Scientific Research Institute, Changjiang Water Resources Commission of the Ministry of Water Resources of China, Wuhan 430015, China*

²*College of Hydrology and Water Resources, Hohai University, Nanjing 210098, China*

³*School of Natural Resources, University of Nebraska-Lincoln, Lincoln, NE 68588, USA*

⁴*Business School of Hohai University, Nanjing 210098, China*

**Corresponding author*

e-mail: wangyq@mail.crsiri.cn; phone: +86-158-5066-0117

(Received 1st Mar 2019; accepted 21st May 2019)

Abstract. Between 25th July and 19th August 2013, Amur River basin received some of its most extreme precipitation on record. The floods caused by the heavy rain brought affected Amur River and its 4 major tributaries. Hailun and Hailar stations break daily maximum precipitation record with 153.6 mm in 30th July, and 85.8 mm in 27th July, respectively. Based on daily precipitation observations at 25 stations from 1954 to 2014, the trends, periodicities and abrupt changes of five extreme precipitation indices in Amur River basin were investigated to the Spatiotemporal Characteristics of the extreme precipitation. Area-averaged annual total wet-day precipitation (PRCPTOT), maximum 1-day precipitation amount (Rx1day), maximum 5-day precipitation amount (Rx5day), very wet days (R95) and extremely wet days (R99) had non-significant trends. By wavelet analysis for annual PRCPTOT, Rx1day, Rx5day, R95 and R99 series, the real part wavelet phase of main periods were mostly located at positive peaks in 2013, which were corroborated by abrupt change analysis. Multi-cycle superimposition of main periods is possibly the main cause for extreme precipitation in 2013. The record-breaking daily precipitation data improve 100-year recurrence interval (111.47 mm) to 130.61 mm in Hailun and raise 100-year recurrence interval from 78.95 mm to 87.91 mm in Hailar.

Keywords: *precipitation extremes trend analysis wavelet analysis abrupt change Amur River basin*

Introduction

Climate change is a severe issue all around the world, which received a lot of attention. The studies in the mean value for temperature and precipitation have made very rich and detailed achievements in different regions, such as China (Qian and Zhu, 2001; Shi et al., 2007), Italy (Moonen et al., 2002), Iran (Tabari and Talaei, 2011), Chile (Kumar et al., 1992), and South Africa (Minetti et al., 2003). The extreme climate events always accompanied by the disasters and the life and property losses directly (Easterling et al., 2000a; Changnon et al., 2000; Griggs and Noguer, 2002), attracts more and more interests of international organizations and scientific research personnel in recent years (Allen et al., 2015; Bordi et al., 2007; Furió and Meneu, 2011). Extreme events, generally defined as the extreme low or high values in the range of observation data (Field et al., 2012), are considered more important and necessary than the study of the mean values referred to human and natural system (Aguilar et al., 2009; Katz and Brown, 1992). As climate changes present poor-rich effects on different regions, the

intensity and frequency of the extreme events also show different variation characteristics on geographically. In particular, the extreme precipitation indices present both negative and positive trends in India (Revadekar and Preethi, 2012; Preethi et al., 2011) and China (Wang and Zhou, 2005; Fu et al., 2013). It is generally that the changes in precipitation is the result of global atmospheric circulation in large spatial and temporal scales (Trenberth, 1999), and easily affected by monsoon (Li and Liu, 2006; Turner and Slingo, 2009), the Arctic Oscillation (Scaife et al., 2008), El Niño (Easterling et al., 2000b; DeFlorio et al., 2013) and other factors in the small term, but the relations between extreme indices and these factors are not the focus in our analyses and detailed research will be considered in future.

As one of the most important international rivers in East Asia with plenty of water, vast area and diversity of ecological features, Amur River has been concerned universally. The main factor caused the 2013 flood is the big amount of moisture poured on the Amur River basin, influenced by the East Asian monsoon, the Siberia High, high-pressure of the Pacific Ocean, the Arctic oscillation (AO) and so on (Danilov-Danil'yan and Gel'fan, 2014). Therefore, it is necessary to explore the spatiotemporal characteristics of the extreme precipitation events and take measures to cut back the damage from the events.

The five extreme precipitation indices were chosen to identify the changes of extreme precipitation events firstly: PRCPTOT, Rx1day, Rx5day, R95 and R99, which were recommended by World Meteorological Organization (WMO), United Nations Environment Programme (UNEP), et al. (Tao et al., 2018; Li et al., 2018). Secondly, the Mann-Kendall test was used to calculate the magnitude of the trends for five extreme indices, and evaluate whether the trend is significant or not. Then the periodicities of the extreme indices were analyzed by wavelet transform, and the abrupt changes were detected by Mann-Kendall method. Compared with the results of the trends and periodicities, the changes of the five extreme indices time series were analyzed, and the changes could partly reveal the causes of the 2013 extreme precipitation. Finally, the extent of the 2013 extreme precipitation was measured by analyzing the typical station, and some conclusions were given. This paper aims to provide a reference for international river-related countries to deal with extreme weather events through the study of extreme precipitation in the Amur River Basin.

Study area and data

Study area

The Amur River (*Fig. 1*), with the other name as Heilong River in Chinese, has the tenth largest basin area on earth (Nicholson et al., 2014). The Amur River basin has an area of 1.86 million km² which covers the territories of Mongolia, Russia, China and North Korea. In addition to its transboundary location, the Amur River basin can be characterized by contrasts between other geographic aspects: Russia and Asia; continental and monsoon climates; and southern dense and northern sparse populations. The climate of eastern Amur basin is humid monsoon temperature climate, which impact can reach the northernmost latitude on earth (Semenov et al., 2014; Yu et al., 2013). The climate of areas in the west of this basin (upper reach of the Amur River) is sheltered from monsoon influence and arid. The arid western portion of this basin is smaller compared with the more humid eastern portion.

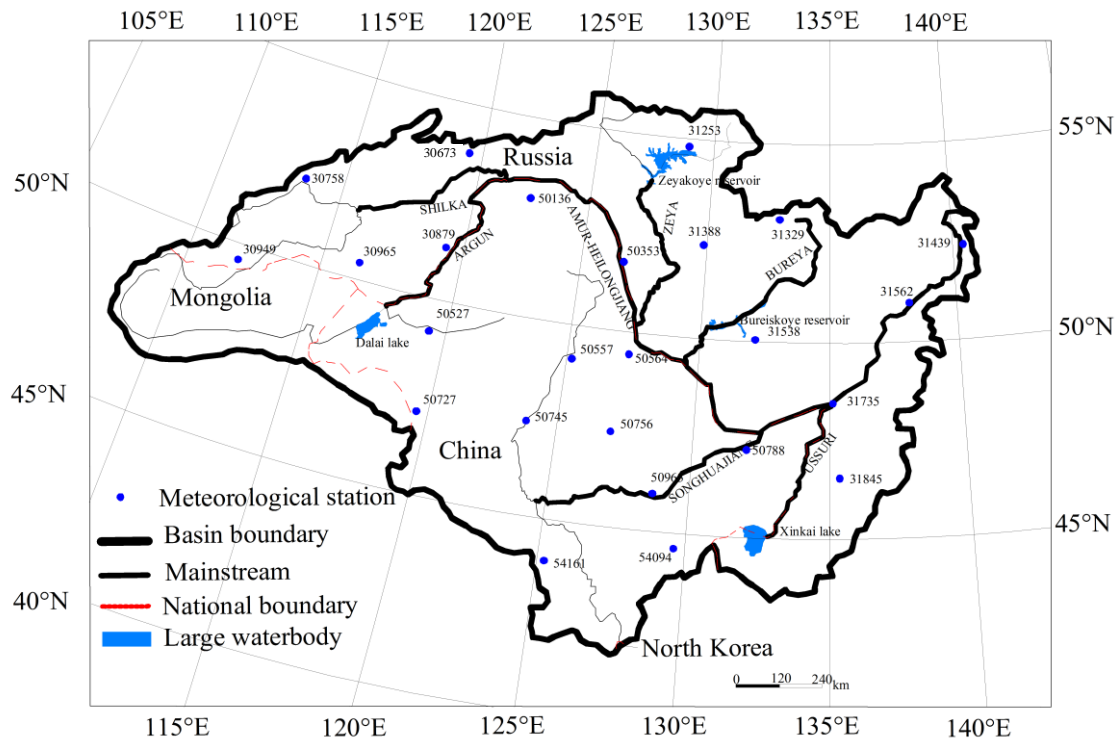


Figure 1. Locations of the 25 meteorological stations in the Amur River basin

Long-term observed precipitation data

The daily precipitation data from 1954 to 2014 were collected in 25 stations of which the 12 stations in China and 13 stations in Russia. *Figure 1* presented the geographical location of the stations and more information were shown in *Table 1*. The Chinese station data was provided from the National Climate Center, China Meteorological Administration, and the station data of Russia came from Russian Federal Service for Hydrometeorology and Environmental Monitoring. The data collected from authoritative departments in China and Russia are measured daily data of meteorological sites. Data quality control is necessary in the calculation and detecting the trends and periodicities of the extreme precipitation indices (Huang et al., 2013; You et al., 2014), although these data has been detected by primary quality control. The RHtestV.4 software package (<http://etcccdi.pacificclimate.org/software.shtml>) was employed for homogeneity assessment (Wang, 2008a, b; Wang and Feng, 2013).

Methodology

In this study, five indices were chosen for variations evaluation of the extreme precipitation in Amur River basin, the definitions of these indices were presented in *Table 2*, and all these indices are from the core indices which were recommended by the Joint CCI-CLIVAR Expert Team for Climate Change Detection Monitoring and Indices (ETCCDMI) and applied in different countries (Liu et al., 2015; Altinsoy et al., 2013). These indices were used widely to study the variations of extreme climate events in many regions of the world.

Table 1. List of 25 stations used in the study

WMO number	Station	Latitude (°N)	Longitude (°E)	Altitude (m)
30673	Mogoca	53.75	119.73	624
30758	Chita	52.08	113.48	671
30879	Nerchinskij Zavod	51.32	119.62	621
30949	Kyra	49.57	111.97	907
30965	Borzja	50.40	116.52	675
31253	Bomnak	54.72	128.87	365
31329	Ekimchan	53.08	132.98	540
31388	Norsk	52.35	129.92	207
31439	Bogorodskoe	52.38	140.47	33
31538	Sutur	50.07	132.13	343
31562	Nizhnetambovskoe	50.93	138.18	20
31735	Habarovsk	48.57	135.17	75
31845	Krasnyj Jar	46.53	135.32	128
50136	Mohe	52.97	122.52	433
50353	Huma	51.72	126.65	177
50527	Hailar	49.27	119.75	610
50557	Nenjiang	49.17	125.23	242
50564	Sunwu	49.43	127.35	235
50727	Aershan	47.17	119.93	997
50745	Qiqihar	47.38	123.92	147
50756	Hailun	47.43	126.97	239
50788	Fujin	47.23	131.98	66
50963	Tonghe	45.97	128.73	109
54094	Mudanjiang	44.57	129.60	241
54161	Changchun	43.90	125.27	237

Table 2. Definitions of five precipitation indices

Index	Indicator name	Definitions	Units
PRCPTOT	Annual total wet-day precipitation	Annual total PRCP in wet days ($RR \geq 1$ mm)	mm
Rx1day	Max 1-day precipitation amount	Monthly maximum 1-day precipitation	mm
Rx5day	Max 5-day precipitation amount	Monthly maximum consecutive 5-day precipitation	mm
R95	Very wet days	Annual total PRCP when $RR > 95$ th percentile	mm
R99	Extremely wet days	Annual total PRCP when $RR > 99$ th percentile	mm

The RCLimDex software was employed to carry out the calculation of extreme precipitation indices. The non-parametric Mann-Kendall test (Ahmad et al., 2015; Yin et al., 2016; Yue et al., 2002) was used to estimate the magnitude of indices trend and verify whether the trend is significant. The Kendall slope is computed as *Equation 1*:

$$\beta = \text{Median}\left(\frac{x_i - x_j}{i - j}\right) \quad (\text{Eq.1})$$

Where $1 < j < i < n$ and β indicates the trend rate, and the unit is mm/year in this study. The threshold of significance test was set to 0.05 when assessing the trends of extreme indices.

Wavelet analysis (Lau and Weng, 1995), as an effective method to detect the periodicity in time series, was used to explore the extreme precipitation indices time series. In this study, Morlet wavelet was as the mother wavelet, to participate in the wavelet transform (Liu et al., 2015; Dai et al., 2003). The original data should be z-score standardized to eliminate the randomness before wavelet transform. The continuous transform is computed as *Equations 2–4*:

$$W_f(a, b) = |a|^{-\frac{1}{2}} \int_{-\infty}^{+\infty} f(t) \overline{\psi}\left(\frac{t-b}{a}\right) dt \quad (\text{Eq.2})$$

$$\psi(t) = e^{ict} e^{-t^2/2} \quad (\text{Eq.3})$$

$$\text{Var}(a) = \int_{-\infty}^{+\infty} |W_f(a-b)|^2 db \quad (\text{Eq.4})$$

Where $f(t)$ is the extreme precipitation indices times series, $W_f(a, b)$ is the coefficient of wavelet transform, a and b are scale and time parameters, respectively. $\psi(t)$ is the morlet wavelet function, and $\text{Var}(a)$ reveals the fluctuations of a in the annual indices series. When $c = 6.2$, the periodicity $T \approx a$, so c was set to 6.2 in this study. By the graph of $\text{Var}(a)$ varying with a , the main periodicities can be marked by the peaks corresponding to a .

The generalized extreme value distribution (GEV) (Furió and Meneu, 2011; Burke et al., 2010), derived from the characterization of extreme event, was employed to fit the annual Rx1day series. The distribution formula is computed as *Equation 5*:

$$G(z; \mu, \theta, \sigma, \xi) = \exp \left\{ - \left[1 + \xi \left(\frac{z - \mu}{\sigma} \right) \right]^{-1/\xi} \right\} \quad (\text{Eq.5})$$

Defined on $\{z: 1 + \xi(z - \mu) / \sigma > 0\}$, $-\infty < \mu < \infty$ (location parameter), $\sigma > 0$ (scale parameter) and $-\infty < \xi < \infty$ (shape parameter). The profile likelihood method is more reasonable to be used to estimate the multi-year return levels and 0.95 confidence intervals, compared with the maximum likelihood method (Huang et al., 2013).

Results and discussion

General characteristics of precipitation extreme indices

The changes of Percentage of precipitation anomalies in the area-averaged time series for five extreme precipitation indices were shown in *Figure 2*, and the basic statistical data was performed in *Table 3*. The changes of 5 indices are almost consistent, while the R99 fluctuate severely. The anomaly percentage of R99 varies from 73.50 to -80.76, while other indices fluctuate between -30 and 30. In particular, the variation coefficient (0.30) of R99 is largest, while PRCPTOT, Rx1day, Rx5day, and R95 are 0.10, 0.08, 0.09 and 0.18, respectively.

Figure 3 shows the distribution for the multi-year mean of extreme precipitation indices from 1954 to 2014 in the Amur River basin. Most of the extreme precipitation events generally occurred in the southeast of the Amur River basin, while the south area

are higher than other area for Rx1day. Spatially, the maximum value of the multi-year mean of extreme precipitation indices generally occurs in the south, while the minimum value generally occurs in the north. Specifically, the maxima of PRCPTOT, R95 and R99 occur in Krasnyj Jar Station (southeast of the basin), and the maxima of Rx1day and Rx5day occur in Changchun Station (southwest of the basin). The minima of PRCPTOT, Rx5day, R95 and R99 occur in Kyra Station (northwest of the basin), and the minimum value of Rx1day occurs in Mogoca Station (northwest of the basin). Particularly, the distributions are similar to the distribution pattern of the annual precipitation in Liu's view, although his study area is just one part of the Amur River basin (Liu et al., 2015).



Figure 2. Percentage of precipitation anomalies changes in the time series for five extreme precipitation indices during 1954 to 2014 (comparison with the averages of 1954~2014). (PRCPTOT-annual total wet-day precipitation, Rx1day-maximum 1-day precipitation amount, Rx5day-maximum 5-day precipitation amount, R95-very wet days, R99-extremely wet days)

Table 3. Statistical information for five extreme precipitation indices time series

Indices	Mean (mm)	Standard deviation	Coefficient of kurtosis	Coefficient of variation	Maxima (mm)	Minima (mm)	Range (mm)	Range/mean (%)
PRCPTOT	500.69	49.16	-0.19	0.10	619.28	399.27	220.01	43.94
Rx1day	46.84	3.86	0.03	0.08	56.26	38.7	17.56	37.49
Rx5day	78.86	7.19	-0.26	0.09	98.79	66.56	32.23	40.87
R95	124.75	22.24	-0.05	0.18	180.88	82.38	98.50	78.96
R99	39.66	11.91	0.54	0.30	68.81	7.63	61.18	154.26

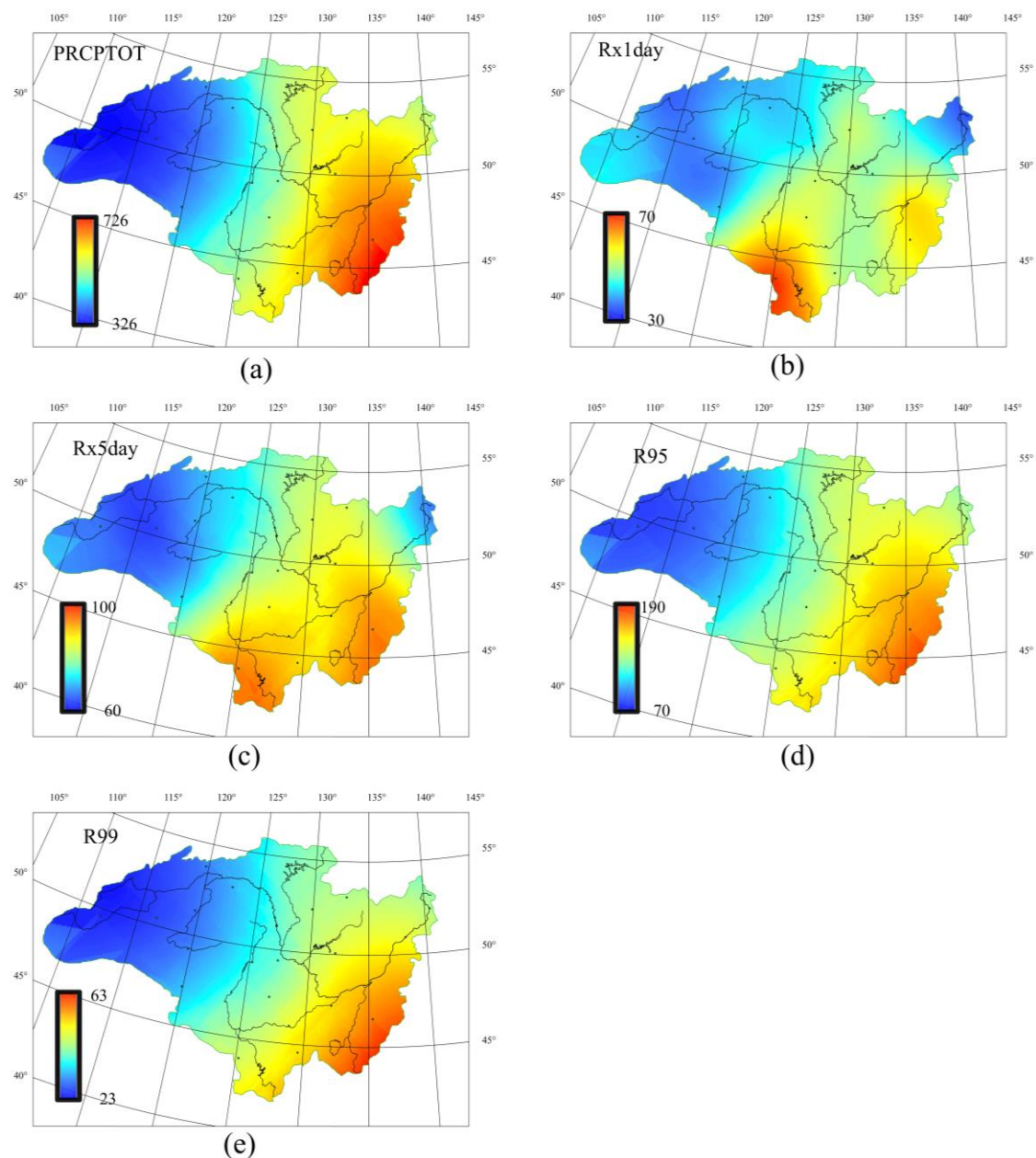


Figure 3. Spatial distribution for the multi-year mean of extreme precipitation indices from 1954 to 2014 in the Amur River basin (unit mm). (PRCPTOT-annual total wet-day precipitation, Rx1day-maximum 1-day precipitation amount, Rx5day-maximum 5-day precipitation amount, R95-very wet days, R99-extremely wet days)

Trends of extreme precipitation indices

For the five indices, the area-averaged trends are weak and statistical non-significant, the Kendall slopes for PRCPTOT, Rx1day, Rx5day, R95 and R99 are -0.28, 0.02, -0.04, 0.01 and 0.09 mm/year, respectively. For the spatial trends results (Fig. 4), only Nizhnetambovskoe station, the trends of Rx1day, Rx5day, R95 and R99 are notable and positive significantly, while the other stations fluctuate weakly in all indices during the study period.

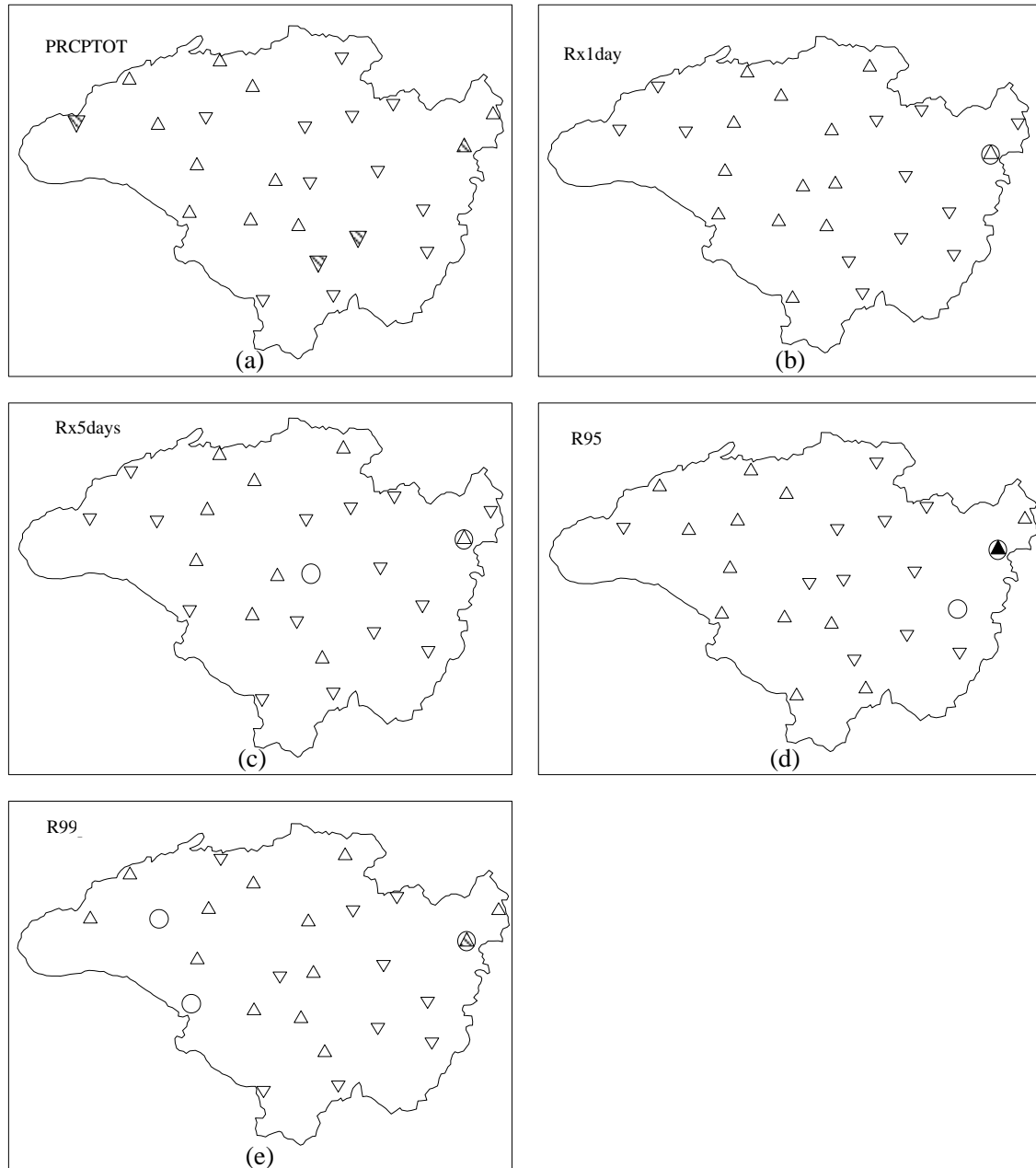


Figure 4. Spatial pattern of trends for the extreme precipitation indices for 25 stations from 1954 to 2014 in the Amur River basin ($\blacktriangle, \triangle, \Delta, \circ, \nabla, \nabla, \nabla$ indicate $\beta > 2$ mm/year, $1 < \beta \leq 2$ mm/year, $0 < \beta \leq 1$ mm/year, $\beta = 0$, $-1 < \beta < 0$ mm/year, $-2 < \beta \leq -1$ mm/year, $\beta \leq -2$ mm/year, respectively; the triangles that are rounded indicate significant trend at 0.05 level). (PRCPTOT-annual total wet-day precipitation, Rx1day-maximum 1-day precipitation amount, Rx5day-maximum 5-day precipitation amount, R95-very wet days, R99-extremely wet days)

Periodicities of extreme precipitation indices

Wavelet analysis is employed to judge the periodicities of the extreme precipitation indices. For PRCPTOT, three peaks can be found in the Periodicities diagnosis graphs of annual area-averaged indices series and they are located at time scale of 4, 13 and 29a. As the peak value means the oscillation strength, the first main period is 29a, and

the second and third are 13 and 4a respectively. The main periods are 30, 19 and 5a for Rx1day, 30, 14 and 6a for Rx5day, 30, 13 and 4a for R95, and 28, 11, 18 and 6a for R99, respectively.

Figure 5 shows the wavelet transform real part variation course of annual area-averaged indices series. The size of amplitude responses the periodic obviousness, and the amplitude of the first main period of 29a are larger than those of 13 and 4a in Figure 5a. For PRCPTOT, the amplitude of 13a time scale becomes gradually smaller in the entire study period, and even weaker than 4a after 1990. It reveals that the periodicity of 4a timescale was more obvious than 13a after 1990. Besides, the positive real part phase means abundant PRCPTOT, while the negative real part phase indicates scarce PRCPTOT. Taking 13a time scale as example, abundant PRCPTOT occurred in 1957-1962, 1969-1974, 1992-1998 and 2010-2014.

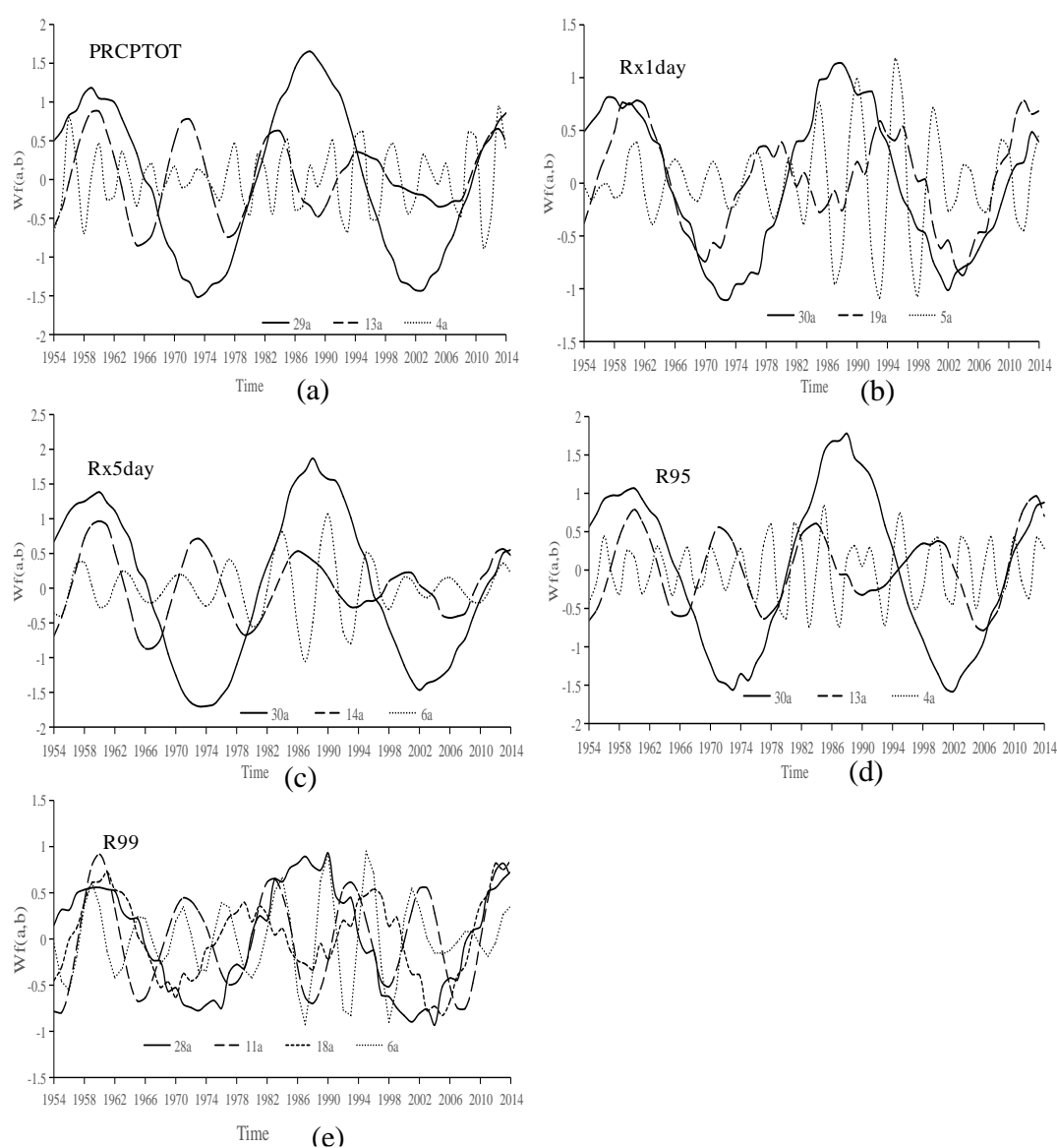


Figure 5. The wavelet transform real part variation course of annual area-averaged indices series (PRCPTOT-annual total wet-day precipitation, Rx1day-maximum 1-day precipitation amount, Rx5day-maximum 5-day precipitation amount, R95-very wet days, R99-extremely wet days)

Overall, the periodicities analysis of the annual extreme precipitation indices explains the cause of the extreme precipitation in Amur River basin in 2013. For PRCPTOT, Rx1day, Rx5day, R95 and R99, the real part wavelet phase of main periods were mostly located at positive peaks in 2013.

Abrupt changes of extreme precipitation indices

The Mann-Kendall method is used to perform abrupt change testing on extreme precipitation indices, which is widely used in hydrometeorology. *Figure 6* shows the Mann-Kendall abrupt change test of the five extreme precipitation indices from 1954 to 2014. It can be seen from the figure that there are similar abrupt change characteristics in the five extreme indices, with two change points around 1963 and around 1989. Both of these change points correspond to the peak of the first main period in *Figure 5*, which indicates that there is a certain relationship between the abrupt change and the periodic variation of the sequence. In addition, the lines of Rx1day, R95 and R99 have intersections in 2013, 2014 and 2012, respectively, while the other two indicators will intersect at the end of the evaluation period, which is almost the same as the peak of the first main period in *Figure 5*.

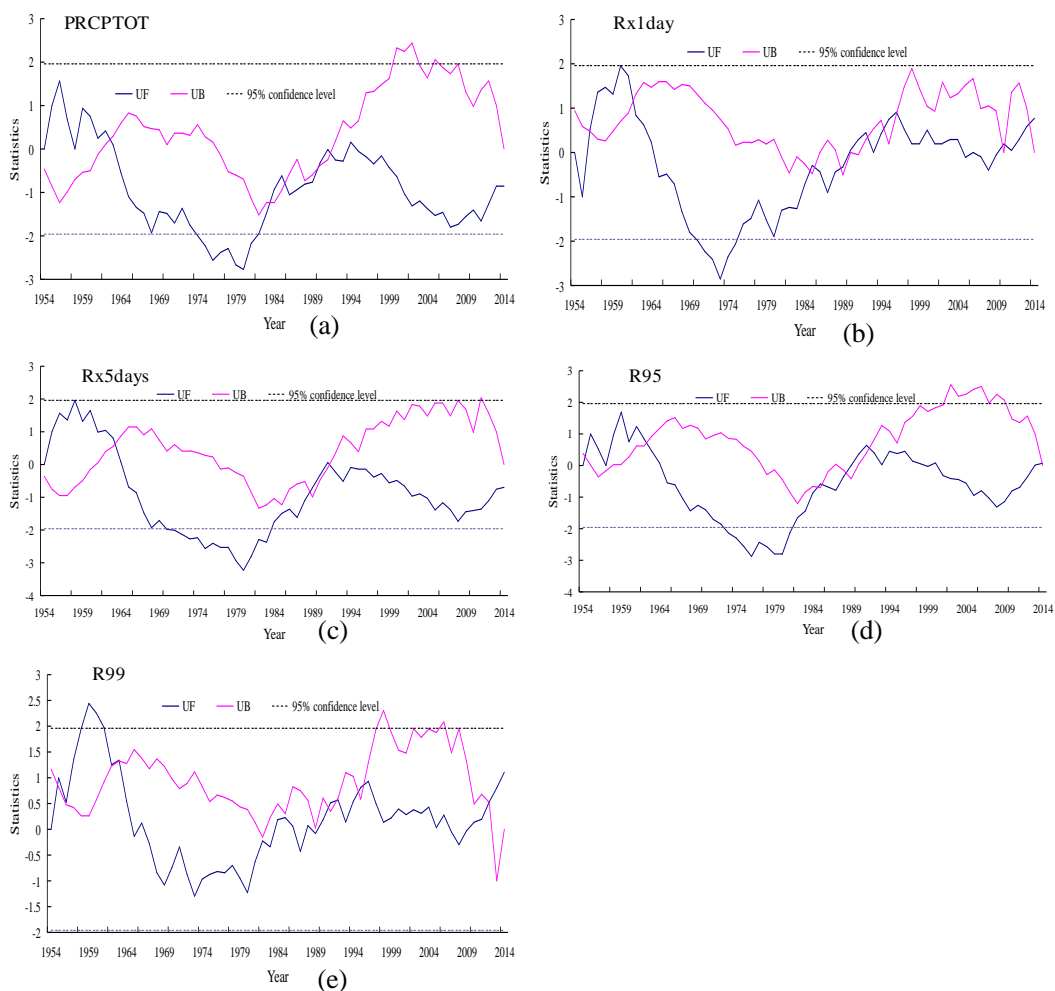


Figure 6. The Mann-Kendall abrupt change test of annual area-averaged indices series. (PRCPTOT-annual total wet-day precipitation, Rx1day-maximum 1-day precipitation amount, Rx5day-maximum 5-day precipitation amount, R95-very wet days, R99-extremely wet days)

Extreme precipitation analyses at typical stations in 2013 floods

The Hailun and Hailar Stations received record-breaking observations of daily maximum precipitation in 2013. The GEV distribution was fitted to the annual Rx1day series of Hailun and Hailar, and the profile likelihood method was employed to estimate the 10/50/100-year return levels (*Table 4*). For Hailun station, the record-breaking data (153.6 mm) was around 100-year return level in the evaluation period of 1954-2012, and improve the 10/50/100-year return levels (76.37, 100.90 and 111.47 mm) to 89.14, 114.62 and 130.61 mm. For Hailar station, the record-breaking observation (85.80 mm) was also around 100-year return level in the period of 1954-2012, and the 10/50/100-year return levels (51.99, 70.45 and 78.95 mm) were raised to 54.21, 76.80 and 87.91 mm.

Table 4. The 10/50/100-year return levels and 0.95 confidence intervals (mm) estimated by the profile likelihood method for annual Rx1day series

Region	Time series	10 years	50 years	100 years
Hailun	1954-2012	76.37(68.63,89.33)	100.90(87.37,136.47)	111.47(94.21,162.38)
	1954-2013	89.14(79.71,97.33)	114.62(94.96,161.45)	130.61(104.34,199.60)
Hailar	1954-2012	51.99(46.51,61.84)	70.45(59.46,101.75)	78.95(64.35,126.00)
	1954-2013	54.21(47.91,65.77)	76.80(63.16,115.72)	87.91(68.94,138.21)

This study analyzes the temporal and spatial variation characteristics of extreme precipitation indices for the trend, periodicity and abrupt change analysis of five extreme precipitation indices. The results of the trend, periodicity and abrupt change analysis are also mutually corroborated, indicating to some extent the correctness of the results of the analysis. This study has certain similarities with the results of other scholars studying Northeast Asia, but other scholars are limited by the availability of data, and the scope of research is limited to China (Deng et al., 2018; Liu et al., 2015) or Russia (Vyshkvarkova and Voskresenskaya, 2018). In addition, some scholars use large-scale meteorological products to analyze extreme precipitation (Zhu et al., 2018; Tao et al., 2018). Based on the analysis of spatio-temporal distribution characteristics of extreme precipitation, this paper uses GEV distribution to analyze the impact of the extremes on the return levels of typical stations by comparison two periods with or without the value of 2013, which is helpful to further understand the numerical value of the single extreme value for the entire evaluation period. Furthermore, the causes of extreme precipitation are not studied in this paper, and it is expected to be demonstrated in future research..

Conclusions

1. Generally, the changes of annual PRCPTOT, Rx1day, Rx5day, R95 and R99 series are almost consistent, while the R99 with the largest variation coefficient (0.30) fluctuate severely.
2. For PRCPTOT, Rx1day, Rx5day, R95 and R99 indices, not only area-averaged but also individual stations have weak and non-significant trends except for the Nizhnetambovskoe Station.

3. It was reasonable to use wavelet analysis to explore the periodicities for annual PRCPTOT, Rx1day, Rx5day, R95 and R99 series, and the real part wavelet phase of main periods were mostly located at positive peaks in 2013. It means that the periodicities of the extreme precipitation indices are the main cause for 2013 extreme precipitation event than the trends.
4. The correlation coefficients among PRCPTOT, Rx1day, Rx5day, R95 and R99 varied from 0.50 to 0.84, and all have passed 0.01 significant level.
5. The Hailun and Hailar stations suffered from record-breaking daily maximum precipitation in 2013, and their 10/50/100-year return levels were raised from 76.37/100.90/111.47 mm and 51.99/70.45/78.95 mm to 89.14/114.62/130.61 mm and 54.21/76.80/87.91 mm, respectively.

Acknowledgements. This work is funded by the National Key R&D Program of China (2017YFC0403600, 2017YFC0403606, 2017YFC1502404), National Public Research Institutes for Basic R&D Operating Expenses Special Project (CKSF2017061/SZ, CKSF2017057/SZ, CKSF2017008), the National Natural Science Foundation of China (No. 51779013, 51509009), Water Conservancy Science and Technology Innovation project of Guangdong Province (2017-03). Special thanks are given to the anonymous reviewers and editors for their constructive comments.

REFERENCES

- [1] Aguilar, E., Barry, A. A., Brunet, M., Ekan, L., Fernandes, A., Massoukina, M., Mbah, J., Mhanda, A. D., Nascimento, D., Peterson, T. (2009): Changes in temperature and precipitation extremes in western central Africa, Guinea Conakry, and Zimbabwe, 1955–2006. – *Journal of Geophysical Research: Atmospheres* (1984–2012) 114(D2).
- [2] Ahmad, I., Tang, D., Wang, T., Wang, M., Wagan, B. (2015): Precipitation trends over time using Mann-Kendall and spearman's RHO tests in swat river basin, Pakistan. – *Advances in Meteorology*. <http://dx.doi.org/10.1155/2015/431860>.
- [3] Altinsoy, H., Ozturk, T., Turkes, M., Kurnaz, M. (2013): Simulating the Climatology of Extreme Events for the Central Asia Domain Using the RegCM 4.0 Regional Climate Model. – In: Helmis, C., Nastos, P. T. (eds.) *Advances in Meteorology, Climatology and Atmospheric Physics*. Springer, Berlin, Heidelberg, pp. 365-370.
- [4] Bordi, I., Fraedrich, K., Petitta, M., Sutera, A. (2007): Extreme value analysis of wet and dry periods in Sicily. – *Theoretical and Applied Climatology* 87(1-4): 61-71.
- [5] Burke, E. J., Perry, R. H. J., Brown, S. J. (2010): An extreme value analysis of UK drought and projections of change in the future. – *Journal of Hydrology* 388(1): 131-143.
- [6] Changnon, S. A., Pielke, R. A., Changnon, D., Sylves, R. T., Pulwarty, R. (2000): Human factors explain the increased losses from weather and climate extremes. – *Bulletin of the American Meteorological Society* 81(3): 437-442.
- [7] Dai, X., Wang, P., Chou, J. (2003): Multiscale characteristics of the rainy season rainfall and interdecadal decaying of summer monsoon in North China. – *Chinese Science Bulletin* 48(24): 2730-2734.
- [8] Danilov-Danil'yan, V. I., Gel'fan, A. N. (2014): The extraordinary flood in the Amur River Basin. – *Herald of the Russian Academy of Sciences* 84(5): 335-343.
- [9] Deflorio, M. J., Pierce, D. W., Cayan, D. R., Miller, A. J. (2013): Western US extreme precipitation events and their relation to ENSO and PDO in CCSM4. – *Journal of Climate* 26(12): 4231-4243.
- [10] Deng, Y., Jiang, W., He, B., Chen, Z., Jia, K. (2018): Change in intensity and frequency of extreme precipitation and its possible teleconnection with large-scale climate index

- over the china from 1960 to 2015. – *Journal of Geophysical Research Atmospheres* 123(4).
- [11] Easterling, D. R., Evans, J. L., Groisman, P. Y., Karl, T. R., Ambenje, P. (2000a): Observed variability and trends in extreme climate events: a brief review. – *Bulletin of the American Meteorological Society* 81(3): 417-425.
- [12] Easterling, D. R., Meehl, G. A., Parmesan, C., Changnon, S. A., Karl, T. R., Mearns, L. O. (2000b): Climate extremes: observations, modeling, and impacts. – *Science* 289(5487): 2068-2074.
- [13] Field, C., Barros, V., Stocker, T. et al. (2012): *Managing the Risks of Extreme Events and Disasters to Advance Climate Change Adaptation. A Special Report of Working Groups I and II of the Intergovernmental Panel on Climate Change.* – Cambridge University Press, New York.
- [14] Fu, G., Yu, J., Yu, X., Ouyang, R., Zhang, Y., Wang, P., Liu, W., Min, L. (2013): Temporal variation of extreme rainfall events in China, 1961–2009. – *Journal of Hydrology* 487: 48-59.
- [15] Furió, D., Meneu, V. (2011): Analysis of extreme temperatures for four sites across Peninsular Spain. – *Theoretical and Applied Climatology* 104(1-2): 83-99.
- [16] Griggs, D. J., Noguer, M. (2002): the scientific basis. Contribution of working group I to the third assessment report of the intergovernmental panel on climate change. – *Weather* 57(8): 267-269.
- [17] Huang, F., Xia, Z., Guo, L., Yang, F. (2013): Climate change detection and annual extreme temperature analysis of the Irtysh Basin. – *Theoretical and Applied Climatology* 111(3-4): 465-470.
- [18] Katz, R. W.; Brown, B. G. (1992): Extreme events in a changing climate: variability is more important than averages – *Climatic Change* 21(3): 289-302.
- [19] Kumar, K. R., Pant, G. B., Parthasarathy, B., Sontakke, N. A. (1992): Spatial and subseasonal patterns of the long-term trends of Indian summer monsoon rainfall. – *International Journal of Climatology* 12(3): 257-268.
- [20] Lau, K. M., Weng, H. (1995): Climate signal detection using wavelet transform: How to make a time series sing. – *Bulletin of the American Meteorological Society* 76(12): 2391-2402.
- [21] Li, C., Walter, L. F., Wang, J., Hubert, F., Mariia, F., Hu, R., Yin, S., Bao, Y., Yu, S., Julian, H. (2018): An analysis of precipitation extremes in the inner mongolian plateau: spatial-temporal patterns, causes, and implications. – *Atmosphere* 9(8): 322.
- [22] Li, J., Liu, B. (2006): The change character of monsoon rainband over Heilongjiang Province for the past 40 years. – *Journal of Forestry Research* 17(1): 71-74.
- [23] Liu, B., Xiao, C., Liang, X. (2015): Evaluation of spatial and temporal characteristics of precipitation variations in Jilin Province, Northeast China. – *Theoretical and Applied Climatology* 122(1-2): 129-142.
- [24] Liu, R., Liu, S., Cicerone, R., Shiu, C., Li, J., Wang, J., Zhang, Y. (2015): Trends of extreme precipitation in eastern China and their possible causes. – *Advances in Atmospheric Sciences* 32(8): 1027-1037.
- [25] Minetti, J. L., Vargas, W. M., Poblete, A., Acuña, L., Casagrande, G. (2003): Non-linear trends and low frequency oscillations in annual precipitation over Argentina and Chile, 1931-1999. – *Atmósfera* 16(2): 119-135.
- [26] Moonen, A. C., Ercoli, L., Mariotti, M., Masoni, A. (2002): Climate change in Italy indicated by agrometeorological indices over 122 years. – *Agricultural and Forest Meteorology* 111(1): 13-27.
- [27] Nicholson, U., Poynter, S., Clift, P. D., Macdonald, D. I. M. (2014): Tying catchment to basin in a giant sediment routing system: a source-to-sink study of the Neogene–Recent Amur River and its delta in the North Sakhalin Basin. – *Geological Society, London, Special Publications* 386(1): 163-193.

- [28] Preethi, B., Revadekar, J. V., Munot, A. A. (2011): Extremes in summer monsoon precipitation over India during 2001–2009 using CPC high-resolution data – *International Journal of Remote Sensing* 32(3): 717-735.
- [29] Qian, W., Zhu, Y. (2001): Climate change in China from 1880 to 1998 and its impact on the environmental condition. – *Climatic Change* 50(4): 419-444.
- [30] Revadekar, J., Preethi, B. (2012): Statistical analysis of the relationship between summer monsoon precipitation extremes and foodgrain yield over India. – *International Journal of Climatology* 32(3): 419-429.
- [31] S. M. Allen, Gough, W. A., Mohsin, T. (2015): Changes in the frequency of extreme temperature records for Toronto, Ontario, Canada. – *Theoretical and Applied Climatology* 119(3-4): 481-491.
- [32] Scaife, A. A., Folland, C. K., Alexander, L. V., Moberg, A., Knight, J. R. (2008): European climate extremes and the North Atlantic Oscillation. – *Journal of Climate* 21(1): 72-83.
- [33] Semenov, E. K., Sokolikhina, N. N., Tatarinovich, E. V., Tudrii, K. O. (2014): Synoptic conditions of the formation of a catastrophic flood on the Amur River in 2013. – *Russian Meteorology and Hydrology* 39(8): 521-527.
- [34] Shi, Y., Shen, Y., Kang, E., Li, D., Ding, Y., Zhang, G., Hu, R. (2007): Recent and future climate change in Northwest China. – *Climatic Change* 80(3-4): 379-393.
- [35] Tabari, H. Talaee, P. H. (2011): Temporal variability of precipitation over Iran: 1966–2005. – *Journal of Hydrology* 396(3): 313-320.
- [36] Tao, Y., Wang, W., Song, S., Ma, J. (2018): Spatial and temporal variations of precipitation extremes and seasonality over China from 1961~2013. – *Water* 10(6): 719.
- [37] Trenberth, K. E. (1999): Conceptual Framework for Changes of Extremes of the Hydrological Cycle with Climate Change. – In: Karl, T. R. et al. (eds.) *Weather and Climate Extremes*. Springer, Dordrecht, pp. 327-339.
- [38] Turner, A. G., Slingo, J. M. (2009): Uncertainties in future projections of extreme precipitation in the Indian monsoon region. – *Atmospheric Science Letters* 10(3): 152-158.
- [39] Vyshkvarikova, E. V., Voskresenskaya, E. N. (2018): Changes of extreme precipitation in Southern Russia. – *IOP Conference Series: Earth & Environmental Science* 107(1): 012044.
- [40] Wang, X., Wang, T., Yang, M., Zhang, N., Lu, D., Xu, T. (2018): Temporal and spatial distribution characteristics of surface vapor pressure and their influencing factors in Weifang. – *Journal of Meteorology & Environment* 34(3): 78-85.
- [41] Wang, X. L. (2008a): Accounting for autocorrelation in detecting mean shifts in climate data series using the penalized maximal t or F test. – *Journal of Applied Meteorology and Climatology* 47(9): 2423-2444.
- [42] Wang, X. L. (2008b): Penalized maximal F test for detecting undocumented mean shift without trend change. – *Journal of Atmospheric and Oceanic Technology* 25(3): 368-384.
- [43] Wang, X. L., Feng, Y. (2013): *RHtestsV4 User Manual*. – Climate Research Division, ASTD, STB, Environment Canada.
- [44] Wang, Y., Zhou, L. (2005): Observed trends in extreme precipitation events in China during 1961–2001 and the associated changes in large-scale circulation. – *Geophysical Research Letters* 32(9).
- [45] Yin, J., Yan, D., Yang, Z., Yuan, Z., Yuan, Y., Wang, H., Shi, X. (2016): Research on historical and future spatial-temporal variability of precipitation in China. – *Advances in Meteorology*. <http://dx.doi.org/10.1155/2016/9137201>.
- [46] You, C. H., Lee, D. I., Kang, M. Y. (2014): Rainfall estimation using specific differential phase for the first operational polarimetric radar in Korea. – *Advances in Meteorology*. <http://dx.doi.org/10.1155/2014/413717>.
- [47] Yu, L., Xia, Z., Li, J., Cai, T. (2013): Climate change characteristics of Amur River. – *Water Science and Engineering* 6(2): 131-144.

- [48] Yue, S., Pilon, P., Cavadias, G. (2002): Power of the Mann–Kendall and Spearman’s RHO tests for detecting monotonic trends in hydrological series. – *Journal of Hydrology* 259(1): 254-271.
- [49] Zhu, J., Huang, G., Wang, X., Cheng, G., Wu, Y. (2018): High-resolution projections of mean and extreme precipitations over china through PRECIS under RCPs. – *Climate Dynamics* 50(11-12): 4037-4060.